Electronic Supplementary Material (ESI) for Chemical Communications.

Supplementary information

Intrinsic blinking of red fluorescent proteins for super-resolution microscopy

Natalia V. Klementieva[a], Anton I. Pavlikov[a], Alexander A. Moiseev[b], Nina G. Bozhanova[c], Natalie M. Mishina[a,c], Sergey A. Lukyanov[a,c,d], Elena V. Zagaynova[a], Konstantin A. Lukyanov[a,c], Alexander S. Mishin*[a,c]

[a] Nizhny Novgorod State Medical Academy, Nizhny Novgorod, Russia
[b] Institute of Applied Physics, Nizhny Novgorod, Russia
[c] Shemyakin-Ovchinnikov Institute of Bioorganic Chemistry, Moscow, Russia
[d] Pirogov Russian National Research Medical University, Moscow, Russia.

*mishin@ibch.ru

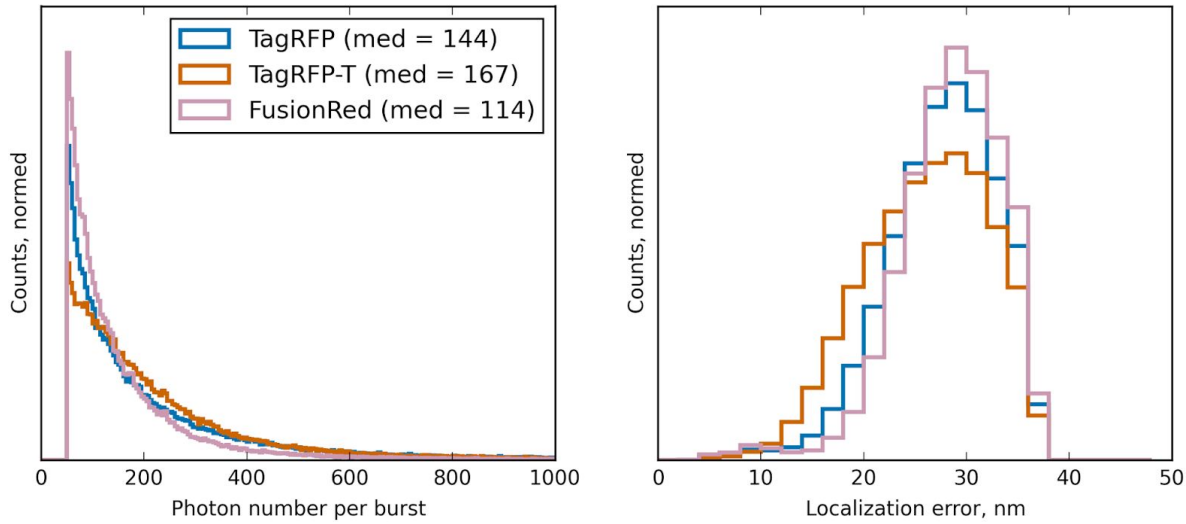

Figure S1. **Photon budget and localization precision.** Left: the photon contents of individual blinking events; right: calculated localization precision. The blinking events were analyzed at sparsely labeled regions of live alpha-actinin labeled cells at the final part of the bleaching series. Imaging conditions: 50 ms camera exposure time and 12.6 W/cm^2 illumination power of the 561-nm continuous laser.

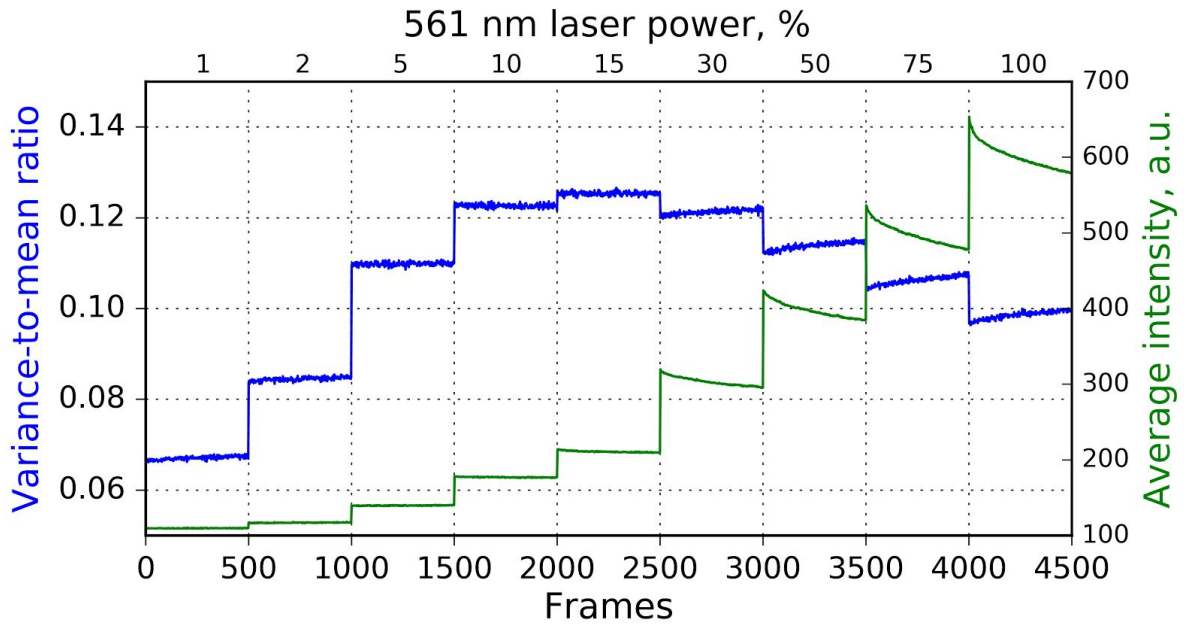

Figure S2. Optimization of imaging conditions. Live HeLa cells transiently expressing TagRFP-T-actinin were imaged under varying laser illumination powers (designated at the top axis). Average pixelwise variance-to-mean ratio computed over two adjustment timepoints over entire frame (256x256 107 nm pixel size, 16 ms exposure time) is shown in blue, average two-frame intensity is shown in green. A representative curve shows incremental increase of the variance-to-mean ratio up to the 10-15% values of the 561 nm laser power (12.6-18.5 W/cm^2). Further increase of the illumination intensity results in the visible contribution of bleaching.

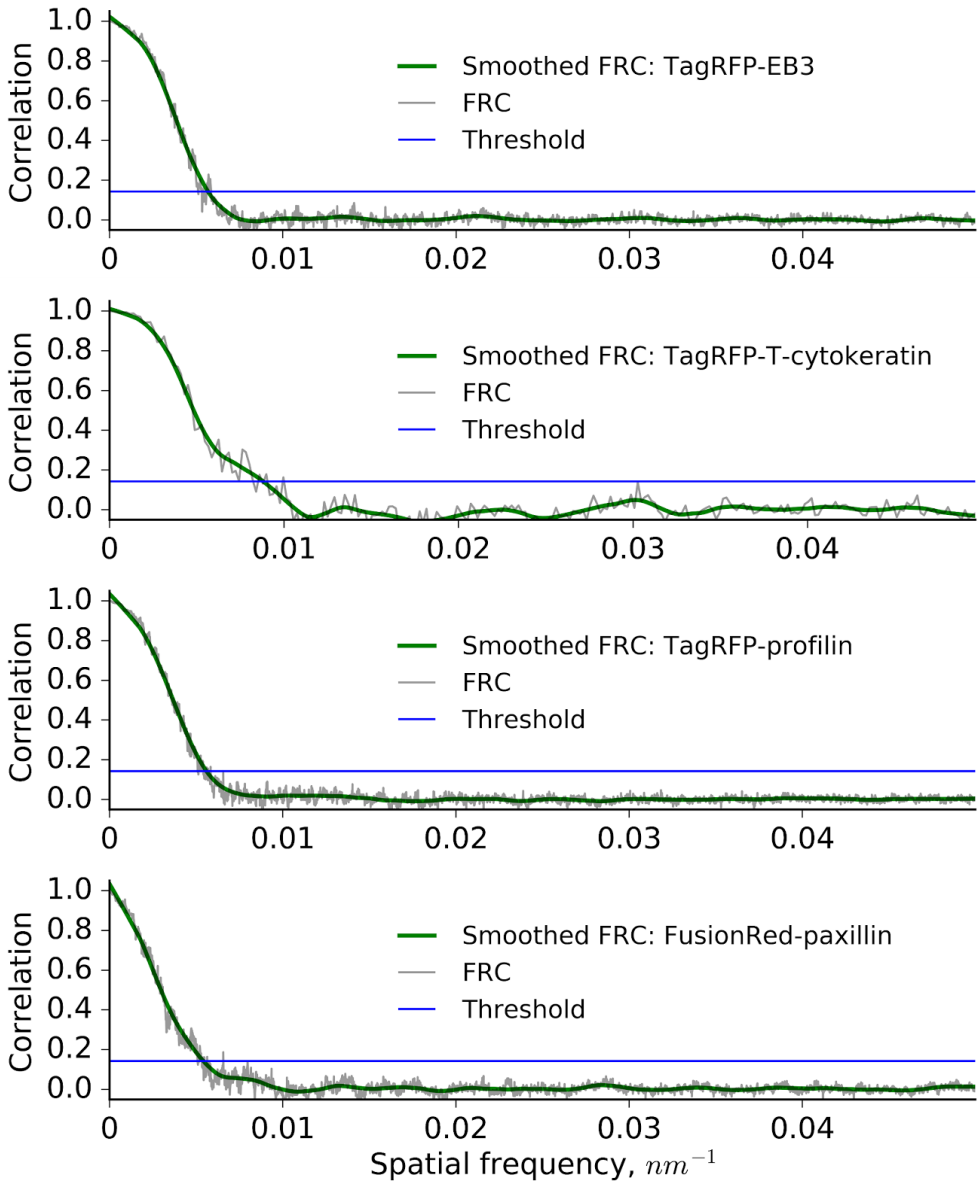

Figure S3. Fourier Ring Correlation (FRC) analysis of the BaLM/gSHRImP reconstruction. The curves correspond to the Figure 1 in the main text and the entire TagRFP-EB3 dataset rendered in the Movie S2. The FRC analysis determines the smallest resolved details in the image. Localizations were split in two halves, rendered separately in the 10-nm pixel grid with 20-nm Gaussian smoothing. The correlation between Fourier transforms of these images over the perimeter of the circle of varying radius in Fourier space results in an FRC curve. The image resolution (FIRE number - Fourier Image REsolution)[1] is defined as the inverse of the spatial frequency for which the FRC curve (correlation value) drops below the fixed threshold (1/7). FIRE values are: 176 nm for TagRFP-EB3, 107 nm for TagRFP-T-cytokeratin, 156 nm for TagRFP-profilin, 186 nm for FusionRed-paxillin.

Methods

Genetic constructs. pTagRFP-actinin, pFusionRed-actinin, TagRFP-profilin, TagRFP-EB3 and pFusionRed-paxillin vectors were from Evrogen. pTagRFP-T-actinin and pTagRFP-T-cytokeratin18 plasmids were constructed by restriction. The TagRFP-T-pQE-30 plasmid (kindly provided by Dr. D. Chudakov) was digested with AgeI/NotI and the coding sequence of fluorescent protein was cloned into pTagRFP-actinin vector to replace TagRFP. Then pTagRFP-T-actinin plasmid was digested with KpnI/NotI and the TagRFP-T with linker sequence at the 5´ end was ligated into KpnI/NotI-digested pmKate2-cytokeratin18 vector (Evrogen).

Cell culture and transient transfection. HeLa and NIH/3T3 cells were grown in Dulbecco's Modified Eagle Media (DMEM) containing 10% fetal bovine serum, 50 U/ml penicillin, 50 μg/ml streptomycin and 4 мM L-glutamine at 37°C and 5% CO_2. Subculturing was performed every 2-3 days, at 80% confluence of culture. For transient transfection and imaging 35 mm Fluorodish™ cell culture dishes (WPI Inc.) were used. Transfections were performed with X-tremeGENE 9 transfection reagents (Roche) according to the manufacturer's instructions. Prior to imaging the cells were washed with phosphate buffered saline (PBS). Live cells were imaged in Minimum Essential Medium Eagle (MEM) (Sigma) without serum.

Imaging. Imaging was carried out on Nikon Eclipse Ti N-STORM microscope with NIS-Elements Software. The samples were focused using 100X oil-immersion objective (Apo TIRF/1.49, Nikon) and PFS (perfect focus system) at an angle allowing for total internal reflection (TIRF). C-NSTORM QUAD filter cube (Nikon, Japan) was used. The sample was continuously illuminated with a green laser (561 nm) in the power range of 6.4-18.5 W/cm^2. Fluorescence emission was collected with an EM-CCD camera (iXon3 DU-897, Andor), exposure time of 16-50 ms, EM gain of 200 or 296, and pre-amplifier gain of 5.1x or 2.4x, respectively. Size of one input pixel was equal to 160 nm/px or 107 nm/px. A series of 100-1000 sequential images were recorded.

Image processing and superresolution image reconstruction. Sparse images of individual fluorophores were fitted in customized Python code utilizing 3D-DAOSTORM [2] software library (https://github.com/ZhuangLab/storm-analysis). Original BaLM [3] algorithm was modified with noise-removing 'running average' step from gSHRImP paper [4]. Briefly, stacks of frames, in groups from 1 to 7, were averaged and subtracted in all possible combinations. The resulting "delta-F-up" and "delta-F-down" stacks were interleaved and fitted with DAOSTORM algorithm. Super-resolution images were rendered in custom Python code by convolving localization centers with 20-nm Gaussian kernel on 10-nm resolution coordinate grid. bSOFI analysis was carried out as described [5] with Balanced SOFI toolbox software. Fourier Ring Correlation[1] analysis of the BaLM/gSHRImP reconstructions was carried out in the Fiji[6] software with the Fourier Ring Correlation Plugin (http://imagej.net/Fourier_Ring_Correlation_Plugin)

Supplementary references

1 R. P. J. Nieuwenhuizen, K. A. Lidke, M. Bates, D. L. Puig, D. Grünwald, S. Stallinga and B. Rieger, *Nat. Methods*, 2013, **10**, 557–562.
2 H. Babcock, Y. Sigal and X. Zhuang, *Optical Nanoscopy*, 2012, 1, 6.
3 D. T. Burnette, P. Sengupta, Y. Dai, J. Lippincott-Schwartz and B. Kachar, *Proc. Natl. Acad. Sci. U. S. A.*, 2011, **108**, 21081–21086.
4 P. D. Simonson, E. Rothenberg and P. R. Selvin, *Nano Lett.*, 2011, **11**, 5090–5096.
5 S. Geissbuehler, N. Bocchio, C. Dellagiacoma, C. Berclaz, M. Leutenegger and T. Lasser, *Optical Nanoscopy*, 2012, 1, 4.
6 J. Schindelin, I. Arganda-Carreras, E. Frise, V. Kaynig, M. Longair, T. Pietzsch, S. Preibisch, C. Rueden, S. Saalfeld, B. Schmid, J.-Y. Tinevez, D. J. White, V. Hartenstein, K. Eliceiri, P. Tomancak and A. Cardona, *Nat. Methods*, 2012, **9**, 676–682.